Angewandte Chemie
Eine Zeitschrift der Gesellschaft Deutscher Chemiker

Supporting Information

Determination of Phase Stability of Elemental Boron**

Mary Anne White, Anthony B. Cerqueira, Catherine A. Whitman, Michel B. Johnson, and Tadashi Ogitsu*

anie_201409169_sm_miscellaneous_information.pdf

We acknowledge the support of NSERC, and Dalhousie University's Institute for Research in Materials and its Facilities for Materials Characterization. A. George provided assistance with synthesis and A. Bent determined some preliminary data. We thank A. Becke, C. Romao, J. Niven, J. Noël, J. Pöhls, P. Scallion and T. Letcher for useful input. The work of T.O. was performed under the auspices of the U.S. Department of Energy by the Lawrence Livermore National Laboratory under Contract No. DE-AC52-07NA27344.

Experimental Methods

Preparation and Characterization of α-Boron

The requirement for α-boron is a sufficiently large sample (*ca*. 50 mg) in one batch for heat capacity measurements. The sample studied here was prepared by the thermal reduction of BCl_3 in a stream of H_2 and Ar gas, at 850 °C (*1*), as shown schematically in Fig. S1. The product deposited on the walls of the quartz tube.

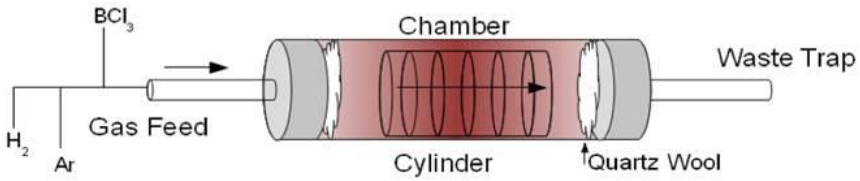

$$2BCl_{3\,(g)} + 3H_{2\,(g)} \longrightarrow 2B_{\,(s)} + 6HCl_{\,(g)}$$

Fig. S1. Chemical vapor deposition set-up to produce α-boron from the reduction of BCl_3.

BCl_3 was from Sigma-Aldrich (99.9%). High-purity H_2 was used to reduce BCl_3, with high-purity Ar as the carrying gas. The reaction was carried out in a quartz cylinder (1 m length, 55 mm OD, 46 mm ID), stuffed at each end with quartz wool, placed in a three-zone radiative furnace (Lindberg 55348). The gas flow, as judged by the bubbler in the exit trap, was *ca*. 1 mL/min. The furnace temperature was maintained at 850 °C for a total run time of 90 minutes, yielding the product, mass *ca*. 30 mg, deposited on the quartz cylinder.

The product was found to be > 99.9% boron (EDS analysis with JEOL 8200 Microprobe; 128 eV resolution) and the structure was confirmed as α-boron by x-ray diffraction (Siemens D500; Cu-K_α; Fig. S2) and Raman spectroscopy (Nicolet NXR 9650; Fig. S3). The latter is especially sensitive to the boron allotrope, with significant differences between α-boron and other allotropes (*2*,*3*).

The synthesized α-boron was a powder and was consolidated by pressing into a pellet with a stainless steel die, at 0.8 GPa for *ca*. 5 min.

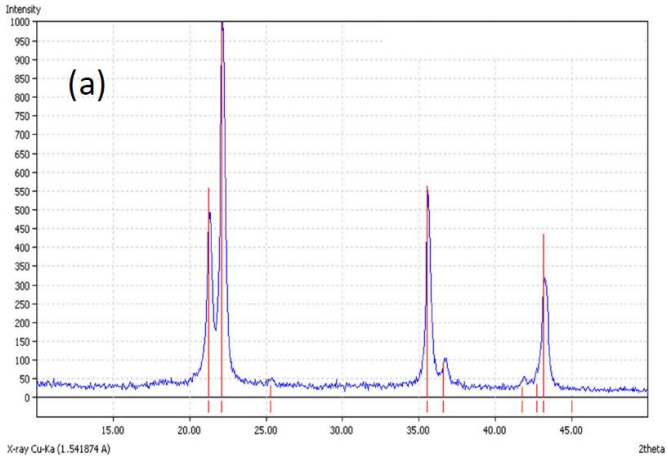

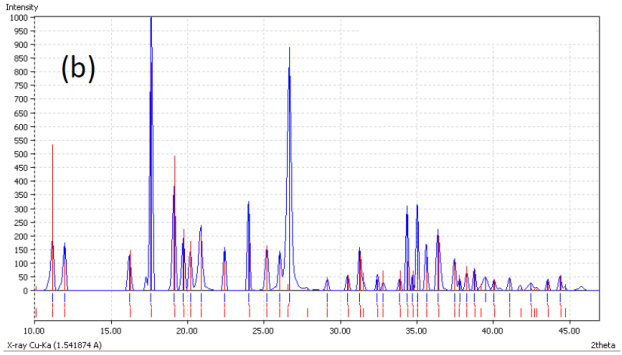

Fig. S2. (a) The experimental x-ray powder diffraction pattern for the α-boron product (**blue**), compared with the experimental powder pattern for α-boron (**red**; literature[4]. (b) The experimental x-ray powder diffraction pattern for the β-boron product (**blue**), compared with the experimental powder pattern for β-boron (**red**; literature[5]).

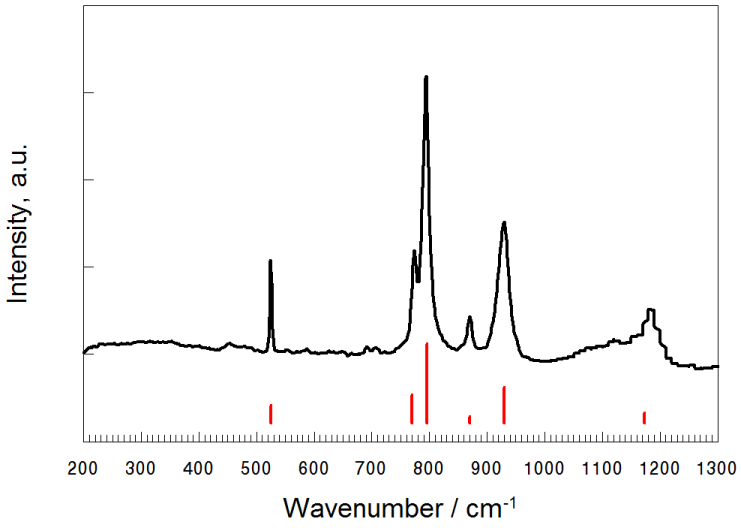

Fig. S3. Raman spectrum of produced α-boron (black), compared with the known Raman-active vibrational frequencies and relative intensities for α-boron (red from Ref. (*2*)).

β-Boron

High-purity (>99.5% pure) β-boron was acquired commercially from Alfa Aesar and used without further purification. The product was found to be > 97% boron (EDS analysis with JEOL 8200 Microprobe; 128 eV resolution) and the structure was confirmed as β-boron by x-ray diffraction (Siemens D500; Cu-K_α; Fig. S2).

Heat capacity measurements required a sample with one flat side (to optimize thermal contact with the calorimeter platform). A shard was freeze-fractured from the main β-boron sample, and then cut into into rectangular prisms on a low-speed Buehler Isomet diamond saw (Lapcraft Dia-Laser #12114 blades).

Heat Capacity Determination

Heat capacity was determined via relaxation calorimetry using a Quantum Design PPMS (San Diego, CA). In this technique a measured quantity of heat is applied to a sample and the temperature response is monitored as a function of time. The setup is shown schematically in Fig. S4. For this study, measurements were taken both with a ^{4}He cryostat and with a ^{3}He cryostat.

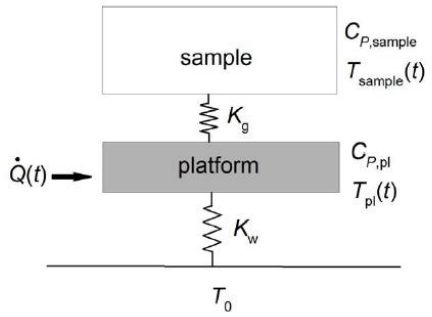

Fig. S4. Schematic of the sample on the platform for a relaxation calorimetry experiment.

When the heater power is discontinued, the temperature of the platform (and anything in perfect thermal contact with it), T_{pl}, decays over time as

$$T_{pl}(t) = T_o + \Delta T e^{-t/\tau_1}, \qquad \text{(S1)}$$

where T_o is the temperature at the time the heater was switched off. The time constant is $\tau_1 = C_{pl} / K_w$ where C_{pl} is the heat capacity of the platform, including anything in perfect thermal contact with it. K_w is the thermal conductance between the platform and the heat-sink via the connecting wires. K_w is determined from a calibration run conducted on a clean platform, with neither sample nor grease on it.

The platform temperature was monitored using the thermometer mounted on the platform underside and it is known (*6*) that

$$C_{pl}\frac{dT}{dt} = -K_w\left(T_{pl} - T_\circ\right) + P(t), \qquad \text{(S2)}$$

where $T_\circ$ is the temperature of the thermal bath (the puck frame), equal to the initial temperature, and $P(t)$ is the power applied by the heater. Therefore, by applying a known quantity of heat and monitoring temperature response, the heat capacity of the platform and all materials in thermal contact with it (including the sample) can be determined from the recorded time versus temperature data. $P(t)$ is equal to the applied heater power when current was passed across the heater (zero otherwise).

The above holds only when the sample is in very good thermal contact with the platform. In general, there is a thermal resistance between the sample and the platform as shown schematically in Fig. S4, where K_w is the thermal conductance between the platform and its surroundings, and K_g is the thermal conductance between the sample and the platform (via the thermal grease).

The temperature of the platform after heating decays with two time constants, τ_1 and τ_2 (hence the name for this method, two-tau), as:

$$T_{pl} = T_0 + A_1\, e^{-t/\tau_1} + A_2\, e^{-t/\tau_2} \qquad \text{(S3)}$$

and the heat capacity of the platform is given by:

$$C_{pl}\left(\frac{dT_{pl}}{dt}\right) = P(t) - K_w\left(T_{pl}(t) - T_0\right) + K_g\left(T_{sample}(t) - T_{pl}(t)\right) \quad \text{(S4)}$$

and that of the sample is given by:

$$C_{sample}\left(\frac{dT_{sample}}{dT}\right) = K_g\left(T_{sample}(t) - T_{pl}(t)\right) \quad \text{(S5)}$$

where thermal coupling constant is quantified as 100 % × $K_g/(K_g+K_w)$. Equations (S3) to (S5) are solved by the PPMS software.

A thermal coupling constant value of 100% indicates perfect thermal contact, while 0% indicates no thermal contact. See below concerning values for acceptable thermal contact in this study.

Thermal contact between the sample and the platform was achieved here using Apiezon® N grease, chosen because it does not have a transition in this temperature range (< 300 K). Since grease was used to make the thermal contact between a sample and the platform, it was necessary to run an addendum heat capacity measurement of the grease alone before an experiment was conducted including a sample. Because heat capacity is an additive property, once both runs had been completed, the addendum could be subtracted from the sample data to give the heat capacity of the sample.

For the most accurate results, the sample heat capacity should contribute no less than 30% of the combined heat capacity of the grease and sample; under these conditions, for thermal insulators, data within 1% of those provided for reference materials can be achieved in the temperature range 5 K < T < 300 K (*7*). There is also potential with relaxation calorimetry for larger samples to give anomalous measurements due to thermal lag within the sample (*7*), and therefore several separate runs were made for samples of different masses for each composition.

The criteria that were examined to ascertain how accurate the heat capacity results are: reproducibility for samples of different masses, the contribution of the sample heat capacity to the total heat capacity, the standard deviation within a triplicate measurement under the same conditions, and the thermal coupling between the sample and the platform; all are discussed in detail below.

Experimental Results

Heat Capacity of α-Boron for T < 300 K

The heat capacity of the synthesized α-boron was determined for four different samples all *ca*. 9 to 10 mg in mass, three samples were determined with the ^{4}He cryostat and one sample with the ^{3}He cryostat. The raw data were assessed and considered robust when the following conditions were met: sample contributes > 25% to the total heat capacity; standard deviation of

triplicate data < 1% for ^{4}He cryostat, < 5% for ^{3}He cryostat; sample coupling to platform > 70%. Although we measured the heat capacity down to *ca*. 0.4 K, only data for $T > 1.8$ K met these criteria because of the exceptionally high value of the Debye characteristic temperature for α-boron (see later). The heat capacity data for the four samples are shown in Figure S5 and tabulated in Appendix A (Tables SA1 to SA4).

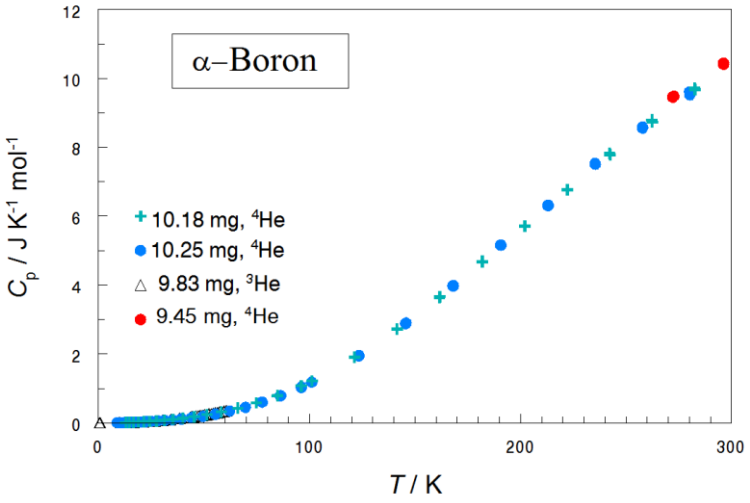

Fig. S5. Experimentally determined heat capacity of α-boron.

The sub-ambient heat capacity of α-boron has been reported previously in the literature as raw data (*8*) and smoothed data from the same lab (*9*). The latter report does not contain experimental details, but the former was by adiabatic calorimetry (sample mass not indicated) which can be inaccurate below *ca*. 60 K (as for β-boron; see below). The two literature data sets diverge above *ca*. 150 K, and also show anomalous behaviour at $T \sim 35$ K (Fig. S6). (Note that another report of the heat capacity of α-boron (*10*) was really for β-boron and that report is not considered further.)

Given the exceptionally low specific heat of α-boron, and the known accuracy of the relaxation calorimeter used here (better than 1% in the range 5 to 300 K, and better than 5% for 0.7 K < T < 5 K (*7*), we conclude that there is no anomaly in the heat capacity of α-boron in around 35 K, and we use only the present data for the further thermodynamic analysis.

The availability of accurate low-temperature heat capacity data for α-boron allows determination of the Debye characteristic temperature, θ_D, from:

$$\lim T \to 0 \quad C_V = \frac{12}{5}\pi^4 Nk \left(\frac{T}{\theta_D}\right)^3 \qquad \text{(S6)}$$

where at very low temperatures $C_V \approx C_P$ is a very good approximation. Because θ_D is so high for α-boron, the fit to equation S6 was confined to T < 3 K, and gave lim T $\rightarrow$0 K θ_D = 850 ± 100 K for α-boron. There was no evidence of an electronic term (γT; $\gamma \sim 0$ here).

(a)

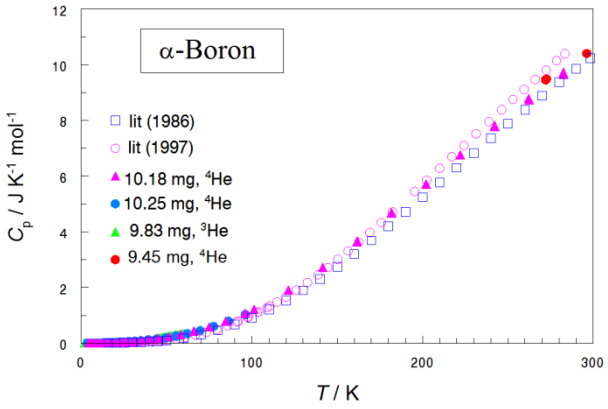

(b)

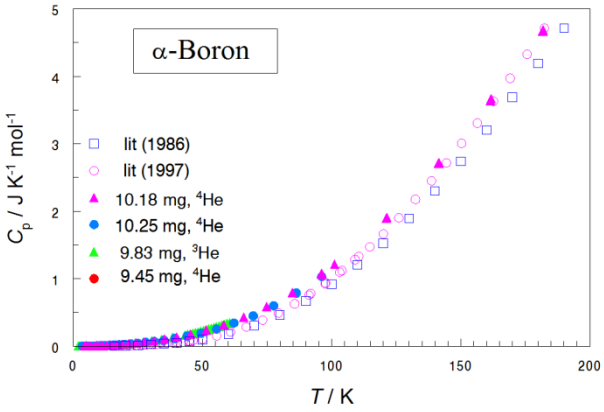

(c)

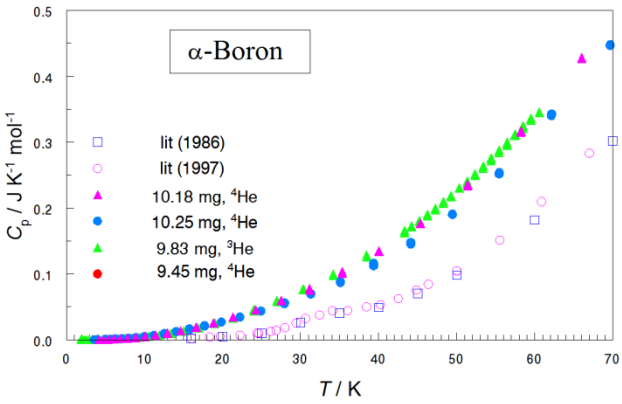

Fig. S6. Literature data (*8*,*9*) for heat capacity of α-boron compared with present experimental data, over various temperature ranges.

Heat Capacity of β-Boron for $T < 300$ K

The heat capacity of β-boron was determined for ten different samples in the range 5 to 35 mg, and all samples were measured in the ^{4}He cryostat. The raw data were assessed and considered robust when the following conditions were met: sample contributes > 20% to the total heat capacity; standard deviation of triplicate data < 1%; sample coupling to platform > 80%. Although we measured the heat capacity down to *ca*. 0.4 K (in the ^{3}He cryostat), only data for T > 2 K in the ^{4}He cryostat met these criteria because of the exceptionally high value of the Debye characteristic temperature for β-boron (see later), and correspondingly low heat capacity. The heat capacity data are shown in Figure S.7 and tabulated in Appendix B (Tables SB1 to SB10).

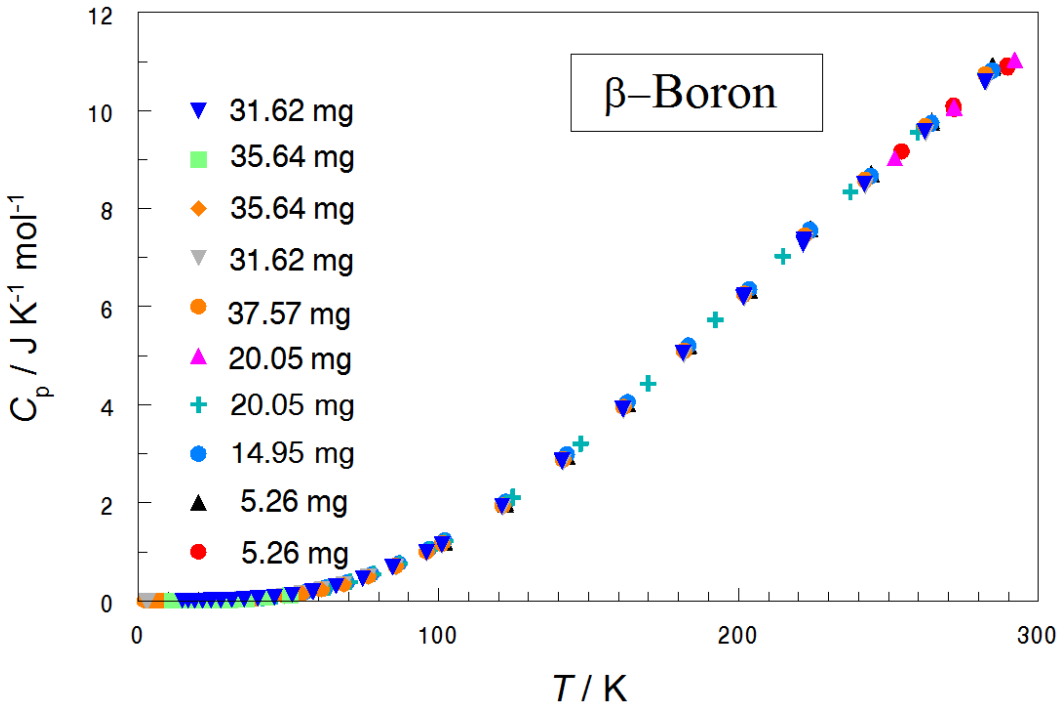

Fig. S7. Experimentally determined heat capacity of β-boron.

The sub-ambient heat capacity of β-boron has been reported previously in the literature, to mixed reviews. The boron data from Magnus and Danz (*11*) were later (*12*) reported to be amorphous boron of unknown purity. Adiabatic calorimetric results for β-boron from 13 to 305 K (*13*) were later reported as inaccurate for T < 60 K (*14*). Smoothed low-temperature heat capacity data of β-boron have been presented without much experimental detail (*15*). Bilir *et al*. (*16*) present low-temperature heat capacity data for β-boron, but only graphically. One other study (*17*), discussed in more detail below, shows unusual behaviour in the heat capacity in the

temperature range 1.3 to 5 K, related to isotopic effects. However, they show the data only in a log-log form so accurate comparison is not possible. Chase (*18*) presents selected assessed data for heat capacity of β-boron over a wide temperature range. The present data are compared with the literature for β-boron in Fig. S8.

For $T > 100$ K, the present data are in good agreement with the original literature (*15, 16, 13*) and assessed data (*18*). At lower temperatures, the present data, which include self-consistent measurements of seven separate samples, are somewhat different from the (reportedly inaccurate) data of Johnston *et al*. (*13*), and the data of Bilir *et al*. (*16*). The latter does not report the methodology and the data were only presented graphically as a smooth curve (no raw data shown) in a conference proceeding. Therefore, we use our data for assessment of thermodynamic quantities of β-boron for $T < 300$ K.

The very low-temperature heat capacity data for β-boron can best be seen in a log-log plot (Fig. S9). As observed by Hu *et al*. (*17*), we find an up-turn in the log-log plot at low temperatures. Hu *et al*. found a dependence of the up-turn on isotope content, and also found C_p to be dependent on magnetic field. We have not investigated the latter here as our main interest is ΔH and ΔS associated with $\int C_p dT$ and $\int C_p T^{-1}\, dT$, respectively, and such differences in the very low values of C_p in this temperature range are insignificant for ΔH and ΔS determination.

However, we did assess the Debye characteristic temperature of β-boron from the C_p data outside the range of the low-temperature anomaly (we used the range 2 to 10 K) and find $\theta_D = 1100 \pm 300$ K for β-boron. Note that there is a strong and unusual temperature dependence for θ_D of β-boron, as it exhibits a peak ($\theta_D \approx 1400$ K at $T = 20$ K).

(a)

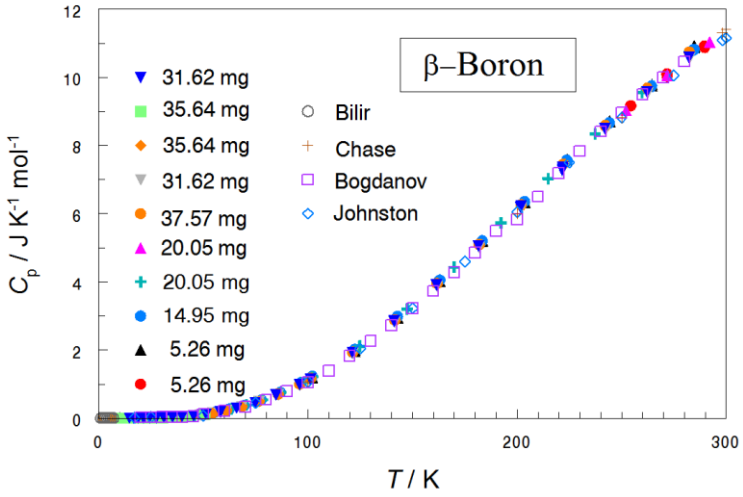
β–Boron
31.62 mg
35.64 mg
35.64 mg
31.62 mg
37.57 mg
20.05 mg
20.05 mg
14.95 mg
5.26 mg
5.26 mg
Bilir
Chase
Bogdanov
Johnston
C_p / J K^{-1} mol^{-1}
T / K

(b)

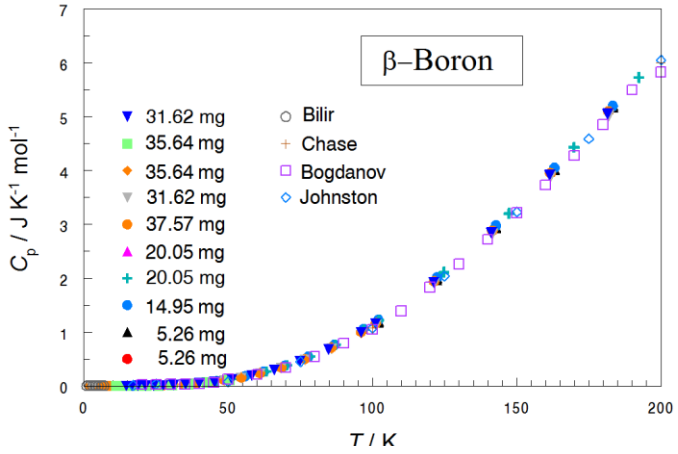
β–Boron
31.62 mg
35.64 mg
35.64 mg
31.62 mg
37.57 mg
20.05 mg
20.05 mg
14.95 mg
5.26 mg
5.26 mg
Bilir
Chase
Bogdanov
Johnston
C_p / J K^{-1} mol^{-1}
T / K

(c)

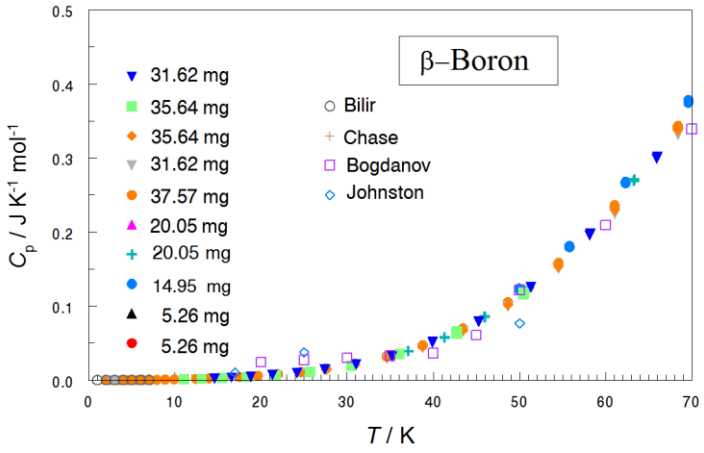
β–Boron
31.62 mg
35.64 mg
35.64 mg
31.62 mg
37.57 mg
20.05 mg
20.05 mg
14.95 mg
5.26 mg
5.26 mg
Bilir
Chase
Bogdanov
Johnston
C_p / J K^{-1} mol^{-1}
T / K

(d)

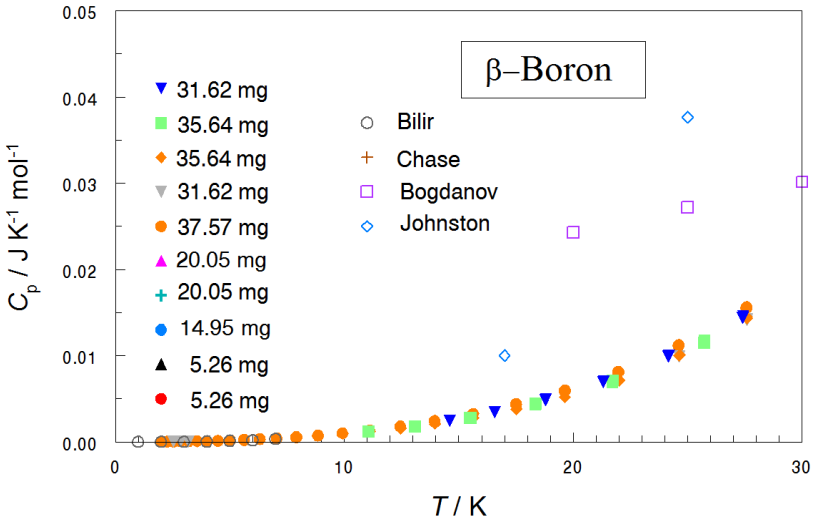

(e)

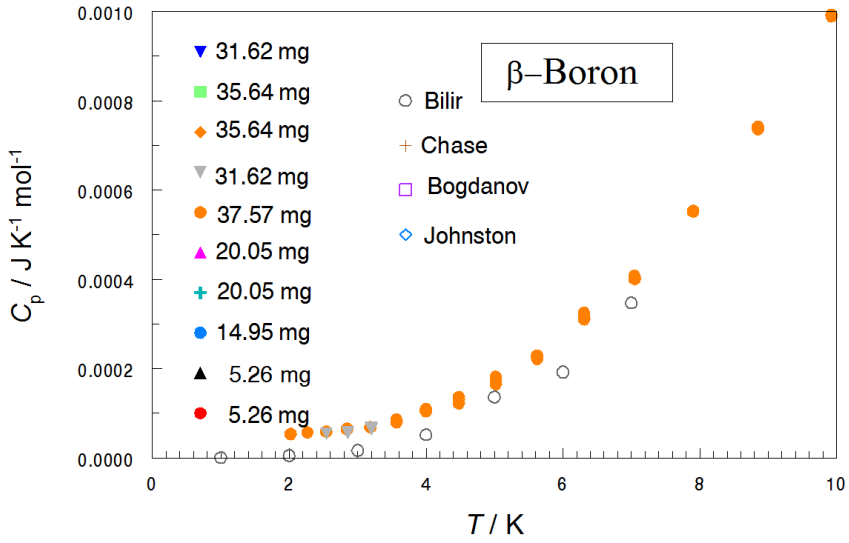

Fig. S8. Literature data for heat capacity of β-boron (see text for references) compared with present experimental data, over various temperature ranges.

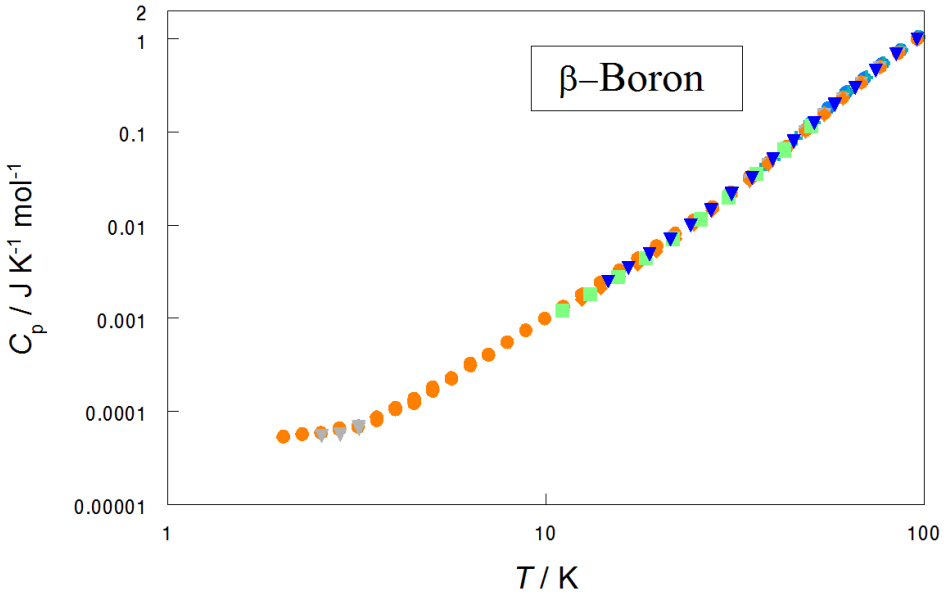

Fig. S9. Closer examination of the present experimental low-temperature heat capacity of β-boron. The legend is the same as for Fig. S8.

Thermodynamic Cycle Analysis

The stability of β-boron in comparison with α-boron has been analyzed using the thermodynamic cycle shown in Fig. S10. Steps 1 and 2 have been achieved through the studies described above. We now consider each of the other steps.

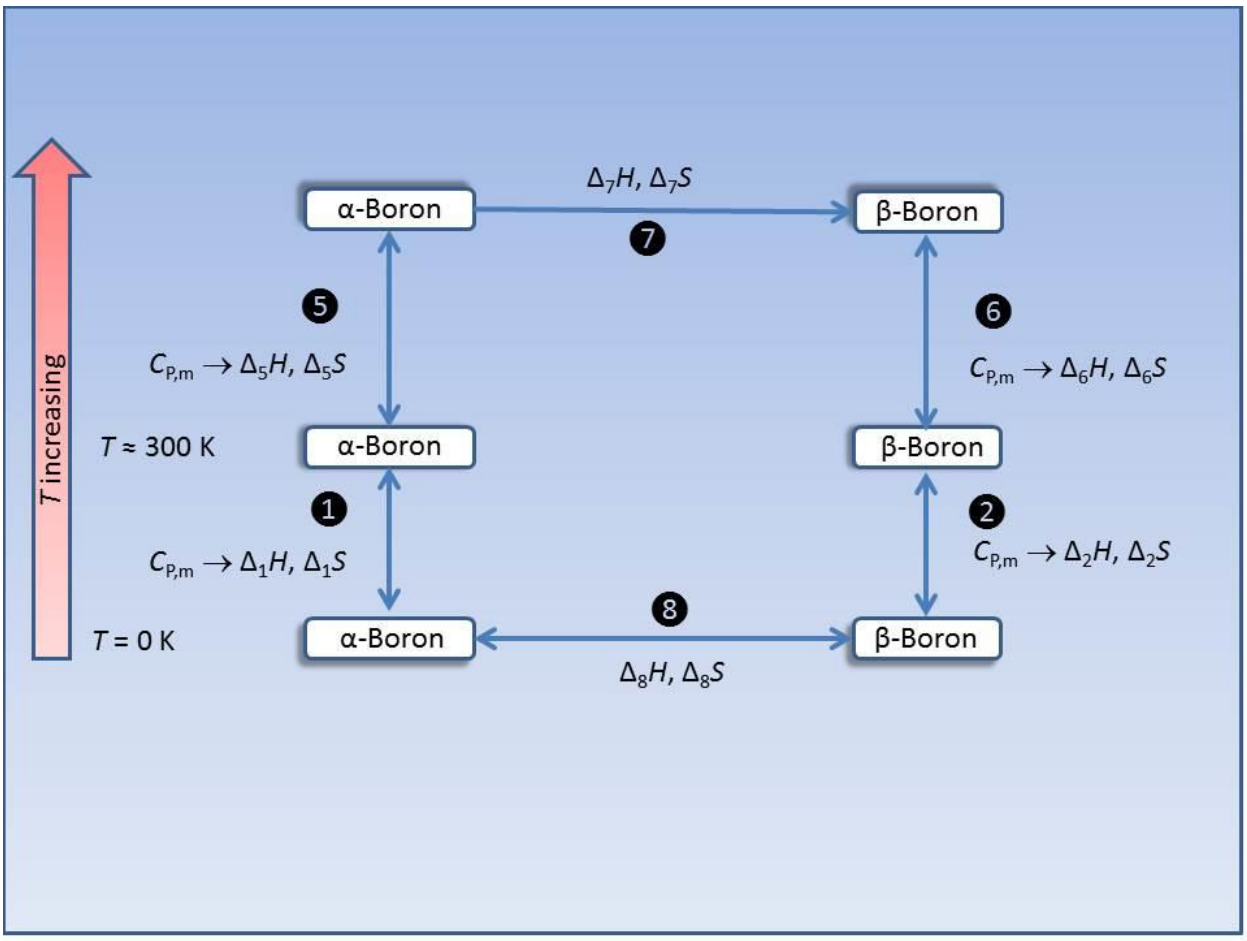

Fig. S10. Thermodynamic cycle to determine relative stability of α- and β-boron. The numbering of the steps is the same as the numbering in the manuscript.

High-Temperature Heat Capacity of β-Boron (Step 6):

The high-temperature (T > 300 K) heat capacity of β-boron has been reported previously. Again, we omit consideration of the boron heat capacity data from Magnus and Danz (*11*) as it was later (*12*) said to be amorphous boron of unknown purity. Wise *et al*.(*19*) and McDonald and Stull (*20*) determined the heat capacity of β-boron by drop calorimetry, from *ca*. 520 K to 1100 K and *ca*. 300 K to 1640 K, respectively. Further drop calorimetry results were reported for the temperature range 1800 K to 2200 K (*21*). Drop calorimetry results from *ca*. 300 K to 800 K also were reported by Jobava *et al*. (*22*) and, although only shown graphically, indicate a strong

isotope dependence (^{11}B has about 15% higher C_p at T = 800 K than ^{10}B). Essentially the same results are also reported elsewhere (*23*), still just graphically. In addition to original data, the high-temperature heat capacity of β-boron has been presented in several assessed data sets (*12*, *18*, *24*). The data sets generally agree quite well (Fig. S11).

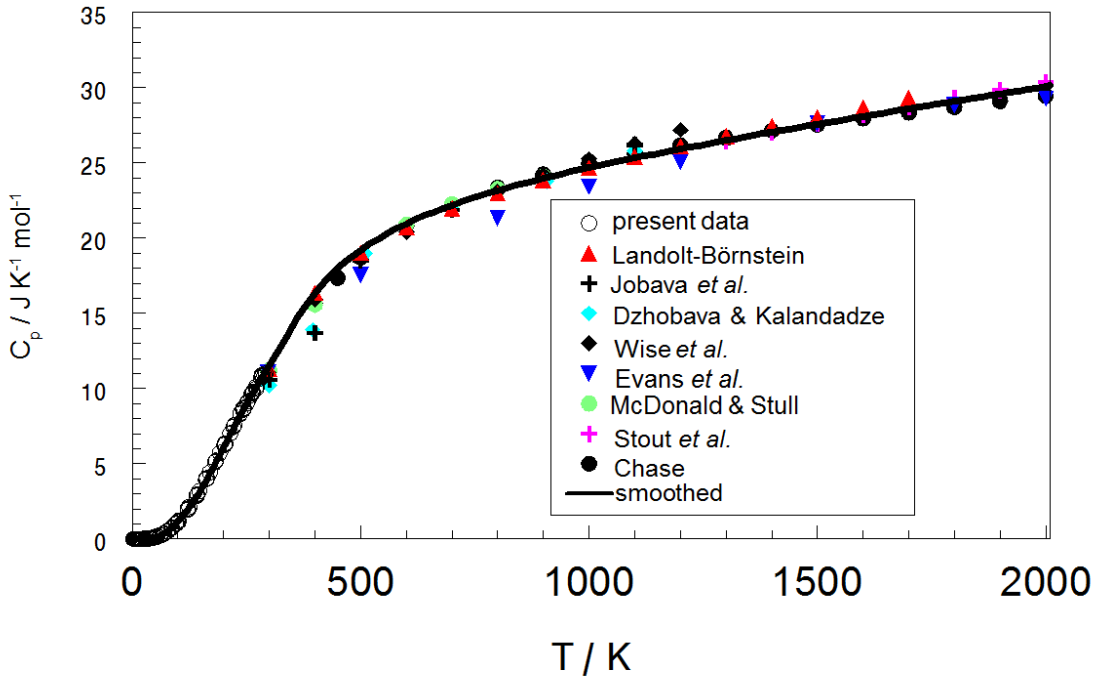

Fig S11. Heat capacity of β-boron as a function of temperature, from various literature sources (see text), and the present data (○) and the smoothed curve used for the chemical thermodynamic analysis.

Hoffmann and Werheit recently reported an anomaly in the heat capacity of β-boron with an onset temperature of 510 K (*25*), which they attributed to hopping of boron atoms between the partially occupied sites. We carried out DSC experiments on β-boron (TA Instruments Q200 DSC; N_2 gas; 10 K min^{-1}; sample mass 13.99 mg) and also saw a subtle anomaly in the same region (Fig S12), and of the same magnitude ($\Delta H \approx 4$ J mol^{-1}). This small anomaly would have been missed with the large step sizes of high-temperature drop calorimetry from the earlier heat capacity studies described above. However, the small associated ΔH is well within the uncertainty of the enthalpy change associated with the main transformation process under consideration, β-boron → α-boron, and does not play a prominent role in the phase stability.

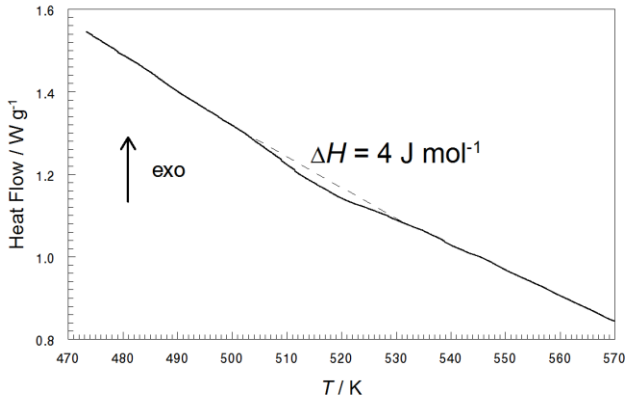

Fig. S12. Present DSC results for 99.5% (Alfa-Aesar) β-boron, showing a subtle thermal anomaly in the region, as previously reported (25).

Fig. S11 summarizes the literature data for the heat capacity of β-boron, along with the present experimental data, and the smoothed curve used to derive ΔH and ΔS for step 6 in the thermodynamic cycle shown in Fig. S10.

High-Temperature Heat Capacity of α-Boron (Step 5):

In contrast with the numerous reports of high-temperature heat capacity for β-boron, there are only a few reports (*22*, *23*, *26*) of super-ambient heat capacity for α-boron, and fewer experimental details published for the reports that are available. Fortunately, two of the reports (*22*, *23*) also give results for β-boron that are in good agreement with other values (see above), which provides a measure of reliability for the results. The available high-temperature heat capacity data for α-boron, along with the present experimental sub-ambient data and the smoothed curve used for integration, are shown in Fig. S13.

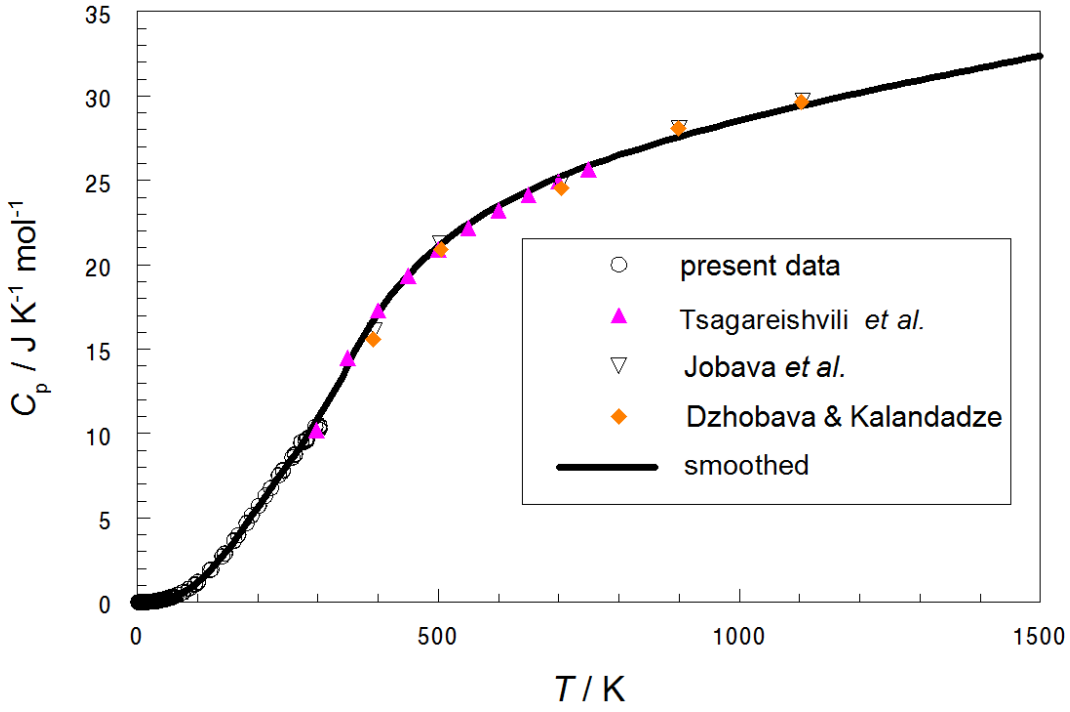

Fig S13. Heat capacity of α-boron as a function of temperature, from various literature sources (see text), and the present data and the smoothed curve used for the chemical thermodynamic analysis.

A major source of uncertainty in the thermodynamic analysis of boron allotropes is that the heat capacity of α-boron has not been determined for temperatures above *ca.* 1100 K, considerably below the temperature of step 7 in the thermodynamic cycle of Fig. S10 (see below). Furthermore, the heat capacity even at 1100 K exceeds the Dulong-Petit value (≈ 25 J K^{-1} mol^{-1}), indicating the importance of anharmonicity in this system at these temperatures, as seen in other systems at high temperatures (*27*,*28*). We have therefore extrapolated the high-T C_p values for α-boron by consideration of the temperature-dependence of C_p of β-boron, as shown in Fig. S14. The extrapolation appears reasonable on the basis of $C_p(T)$ for Si and graphite (*29*) and uncertainties associated with the extrapolation are considered more fully below.

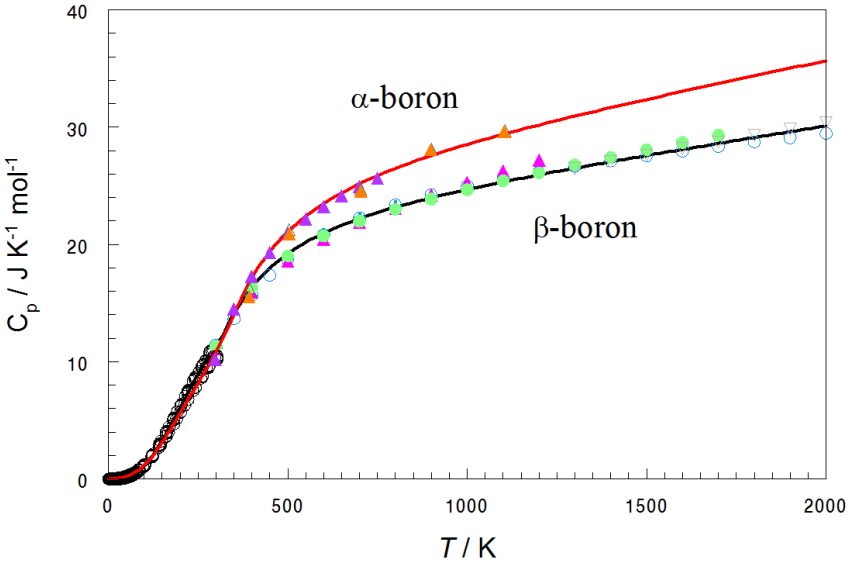

Fig S14. Heat capacities of α-boron and β-boron as functions of temperature, showing the high-temperature extrapolation for α-boron. The legend for the sources of the experimental data is shown on Figs. S11 and S13.

Conversion of α-Boron to β-Boron at High Temperature (Step 7):

It has been known for some time that α-boron converts, via a multi-step process, to β-boron on heating (*30*). The thermodynamics of transformation of α-boron (produced itself by heating of pyrolytic amorphous boron) were investigated using high-temperature DSC (Setaram HT-1500) at suitably high heating rates (3 K min^{-1}) to achieve accurate enthalpy changes (ΔH), consecutively -0.55±0.08 kJ mol^{-1} (α→Int I at 1420 ºC), -1.21±0.17 kJ mol^{-1} (Int I→Int II at 1660 ºC), -4.415±0.055 kJ mol^{-1} (Int II→β at 1710 ºC) (*31*). Those experiments were replicated with different sample masses in the range 30 to 170 mg, and the uncertainty values quoted are standard deviations. We consider ΔH(α→β) to be the sum of the transitions, *i.e.*, -6.18±0.31 kJ mol^{-1}. Furthermore, we take the temperature of step 7 in the thermodynamic cycle of Fig. S10 to be 2013 K (the temperature of completion of the final step in the α→β conversion).

Assessing $\Delta H(\alpha \rightarrow \beta)$ as a Function of Temperature:

From the sub-ambient heat capacities associated with α-boron and β-boron, we can assess the corresponding enthalpy changes for steps 1 and 2, respectively, in the thermodynamic cycle via:

$$\Delta H = \int_{T_1}^{T_2} C_p \, dT \qquad \text{(S.7)}$$

and similarly for the high-temperature enthalpy changes associated with steps 5 and 6. We have the enthalpy change from step 7 from direct measurement in the experiments described above (*31*). Therefore, we can complete the cycle (ΔH(cycle) = 0 since H is a state function) and determine $\Delta H(\alpha \rightarrow \beta)$ at any temperature.

Note that a recent study (32) carried out an integration of the literature heat capacities of α-boron and β-boron and calculated what they called "$(G_\alpha\text{-}G_\beta)^{\text{thermal}}$" = $\int_{T=0}^{T} C_{P,\alpha} \, dT$ - $\int_{T=0}^{T} C_{P,\beta} \, dT$. However, this function is actually only $\Delta H(\beta \rightarrow \alpha) = H_\alpha\text{-}H_\beta$, and only then if $H_\alpha(T{=}0) = H_\beta(T{=}0)$.

Assessing $\Delta S(\alpha \rightarrow \beta)$:

For each of steps 1, 5, 6 and 2 in the thermodynamic cycle of Fig. S10, the corresponding entropy change is

$$\Delta S = \int_{T_1}^{T_2} \frac{C_p}{T} dT. \qquad \text{(S8)}$$

Step 7 in the cycle is a transformation for which we know ΔH (see above), but it is not an equilibrium transition (*i.e.*, $\Delta_7 G \neq 0$) and therefore $T\Delta_7 S \neq \Delta_7 H$. However, step 7 is spontaneous, so $\Delta_7 G < 0$ and therefore $T\Delta_7 S > \Delta_7 H$. Thus, we have a lower bound on $\Delta_7 S$.

From the thermodynamic cycle of Fig. S10, knowledge of $\Delta_1 S$, $\Delta_5 S$, $\Delta_6 S$ and $\Delta_2 S$ would directly give $\Delta_8 S$, *i.e.* the difference in entropy between α-boron and β-boron at $T = 0$, if $\Delta_7 S$ were known quantitatively (since S is a state function and therefore ΔS(cycle) = 0). However, we only know a lower bound on $\Delta_7 S$, and therefore know only an upper bound on $\Delta_8 S$ (= $S(\alpha)\text{-}S(\beta)$ at $T = 0$ K). Given that α-boron is a fully ordered structure, we expect its residual entropy to be zero, *i.e.* $S_0(\alpha) = 0$. Therefore, we can determine a lower bound on the residual entropy of β-boron, $S_0(\beta)$. For the full thermodynamic cycle ($\alpha \rightarrow \beta$), we can determine a lower bound on $\Delta S(\alpha \rightarrow \beta)$, which, since T is always positive, corresponds to an upper bound on $-T\Delta S(\alpha \rightarrow \beta)$ at any given temperature.

Note that this analysis shows very different results from a calculation based only on configurational contributions to the entropy (*32*), showing the important contribution of thermally excited phononic modes to the entropy difference between α-boron and β-boron.

Assessing $\Delta G(\alpha \rightarrow \beta)$:

Although we know definitive values of $\Delta H(\alpha \rightarrow \beta)$ at all temperatures, and can assess $\Delta G(\alpha \rightarrow \beta)$ from:

$$\Delta G = \Delta H - T\,\Delta S \qquad \text{(S9)}$$

we only know an upper bound on $-T\Delta S(\alpha \rightarrow \beta)$, and therefore have an upper bound on $\Delta G(\alpha \rightarrow \beta)$.

Uncertainty Analysis and Limitations of the Investigation:

It is inextricable that the present analysis only allows an upper bound on $-T\Delta S(\alpha \rightarrow \beta)$ and $\Delta G(\alpha \rightarrow \beta)$ but we can still make an estimate of uncertainty on those bounds, and on $\Delta H(\alpha \rightarrow \beta)$.

The two largest sources of uncertainty originate with the extrapolation of the high-temperature heat capacity of α-boron, and the experimental uncertainty associated with the enthalpy change for the high-temperature transformation. (By comparison, uncertainty in sub-ambient C_p contributes negligibly to overall uncertainty.) The uncertainty in $\Delta_7 H$, as discussed above, is 0.31 kJ mol^{-1}. Similarly, based on the high-temperature behaviour of C_p of β-boron and other elements, we consider that the high-temperature extrapolation of $C_p(\alpha)$ could lead to a maximum uncertainty in $H\text{-}H_0$ for α-boron at its high temperature transformation, of about 0.5 kJ mol^{-1}. While, on their own, the enthalpy uncertainties in step 7 (2.1%) and step 5 (*ca*. 1%) are quite small, the values of $\Delta H(\alpha \rightarrow \beta)$ at any point in the cycle arise from small differences between large numbers. Through standard propagation of error, the results shown in the manuscript take account of such uncertainties at all temperatures. All uncertainties presented in the manuscript are at 95% confidence levels.

An additional potential source of uncertainty that we have considered is the influence of isotopic content on the results. Boron is normally *ca*. 80% ^{11}B and 20% ^{10}B, and it is feasible that the CVD preparation of α-boron could lead to a different isotopic composition from the β-boron. The heat capacity of isotopically modified single crystals of β-boron has been determined for 0.5 K < T < 100 K (*17*). Their experimental results show that the heat capacity is essentially independent of isotopic composition for 5 K to 100 K. Below 5 K there are some subtle differences, but any influence of isotopic composition should be negligible for the ΔH and ΔS arguments in the present study.

Also, the particle size could play a role in relative thermal stability. For example, in TiO_2, the relative stability of the bulk polymorphs is different from nanocrystalline TiO_2 (*33*). The surface energetics of various boron allotropes have been calculated (*34*). However, our particle sizes are in the micron range for both α-boron and β-boron, so our conclusions pertain to bulk boron.

Clapeyron Equation Analysis of the Transformation at High Pressure

Experimental investigations of the phase transformations of boron under applied pressure (*2*) show the α-β equilibrium conditions for boron as a function of temperature and pressure. For a single-component system in which two phases are in equilibrium, the Clapeyron equation provides the following relationship:

$$\frac{dP}{dT} = \frac{\Delta_{trs}S}{\Delta_{trs}V} = \frac{\Delta_{trs}H}{T_{trs}\Delta_{trs}V} \qquad \text{(S10)}$$

where the transition entropy, enthalpy and molar volume changes are, respectively, $\Delta_{trs}S$, $\Delta_{trs}H$ and $\Delta_{trs}V$, and P and T refer to the pressure and temperature along the two-phase equilibrium line. We know that α-boron and β-boron coexist (*2*) at (T =1850 K, P = 8 GPa) and (T = 1400 K, P = 4 GPa), and $\Delta_{trs}V$ can be approximated from the densities of the two forms at ambient conditions (*35*), assuming compressibility effects to be negligible. Using an average temperature of transition (T_{trs}) of 1600 K gives $\Delta_{trs}H$ = 3.5 kJ mol^{-1} at P ~ 6 GPa. Although the boron phase diagram of Parakhonskiy *et al*. has been disputed by Qin *et al*. (*36*), the former is very similar to the most recent determination of Ekimov *et al*. (*37*). The latter dP/dT equilibrium curve gives $\Delta_{trs}H$ = 2.6 kJ mol^{-1} for the transition α-boron → β-boron.

On the basis of experiments carried out at P > 4 GPa, Parakhonskiy *et al*. (2) linearly extrapolated their α-β phase equilibrium line and concluded that α was the stable phase of boron at ambient conditions (see Fig. S15). A reasonable extrapolation to P = 0 that leads to β-boron as the stable phase for P = 0 at all temperatures up to 2000 K (Fig. S15) gives, at low temperatures and pressures, dT/dP ~ ∞. The latter implies, via the Clapeyron equation, that $\Delta H(\alpha \rightarrow \beta) \sim 0$ at low temperature and pressure, as we see from our thermodynamic cycle (Fig. 3 of the manuscript), and has been shown also from theoretical studies (*38*).

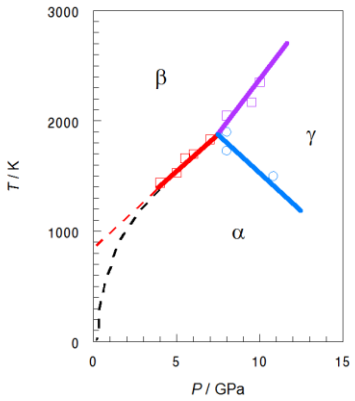

Fig S15. High-pressure boron phase diagram with data from Ref. (*2*), including their linear extrapolation of the α-β phase equilibrium to P = 0 (- - -). Extrapolation of the α-β transition to P = 0 that does not cut the T axis is shown as (- - -). See the main manuscript for details concerning the model for $P \rightarrow 0$.

Appendix A: Heat Capacity of α-Boron.

Table SA1. Heat capacity of α-Boron. Sample mass of 9.45 mg; ^{4}He cryostat. Data in order of measurement.

T/K	C_p/J K^{-1} mol^{-1}
272.72	9.49
272.18	9.47
272.18	9.45
296.17	10.4
296.26	10.4
296.28	10.4

Table SA2. Heat capacity of α-Boron. Sample mass of 9.83 mg; ^{3}He cryostat. Data in order of measurement.

T/K	C_p/J K^{-1} mol^{-1}	T/K	C_p/J K^{-1} mol^{-1}	T/K	C_p/J K^{-1} mol^{-1}	T/K	C_p/J K^{-1} mol^{-1}	T/K	C_p/J K^{-1} mol^{-1}
60.64	0.345	50.34	0.231	30.33	0.0764	9.40	0.00371	2.92	0.000116
60.57	0.346	50.36	0.231	30.37	0.0767	9.40	0.00369	2.92	0.000116
59.54	0.333	49.32	0.217	26.98	0.0598	8.37	0.00277	2.60	0.000084
59.50	0.335	49.28	0.218	26.99	0.0586	8.36	0.00272	2.60	0.000077
59.52	0.337	49.30	0.219	27.02	0.0578	8.37	0.00272	2.60	0.000076
58.50	0.321	48.31	0.207	24.02	0.0462	7.45	0.00202	2.31	0.000058
58.48	0.324	48.27	0.208	24.04	0.0446	7.44	0.00199	2.31	0.000052
58.51	0.325	48.29	0.210	24.05	0.0440	7.44	0.00197	2.31	0.000053
57.47	0.310	47.29	0.197	21.33	0.0336	6.62	0.00143	2.05	0.000040
57.47	0.312	47.25	0.199	21.34	0.0331	6.62	0.00140	2.05	0.000035
57.51	0.312	47.27	0.200	21.36	0.0331	6.61	0.00150	2.05	0.000035
56.46	0.295	46.27	0.188	19.05	0.0254	5.89	0.00108	1.83	0.000026
56.43	0.298	46.23	0.189	19.03	0.0243	5.89	0.00102	1.83	0.000026
56.46	0.300	46.24	0.191	19.03	0.0241	5.89	0.00102	1.83	0.000025
55.44	0.284	45.25	0.179	16.93	0.0183	5.24	0.000738		
55.40	0.286	45.21	0.180	16.92	0.0176	5.24	0.000744		
55.43	0.288	45.23	0.181	16.92	0.0176	5.24	0.000727		
54.41	0.272	44.23	0.171	15.05	0.0136	4.66	0.000536		
54.39	0.275	44.20	0.171	15.05	0.0133	4.66	0.000507		
54.42	0.276	44.21	0.173	15.06	0.0132	4.66	0.000519		
53.41	0.260	43.32	0.166	13.38	0.0100	4.15	0.000372		
53.36	0.262	43.33	0.163	13.37	0.00979	4.14	0.000370		
53.39	0.264	43.29	0.162	13.38	0.00960	4.14	0.000369		
52.39	0.249	38.46	0.129	11.90	0.00723	3.69	0.000266		
52.34	0.250	38.48	0.127	11.89	0.00714	3.69	0.000245		
52.37	0.252	38.48	0.126	11.90	0.00712	3.69	0.000247		
51.37	0.238	34.19	0.100	10.58	0.00539	3.29	0.000177		
51.33	0.239	34.20	0.0980	10.58	0.00516	3.28	0.000170		
51.35	0.241	34.21	0.0973	10.59	0.00518	3.28	0.000171		
50.32	0.230	30.28	0.0763	9.41	0.00381	2.92	0.000122		

Table SA3. Heat capacity of α-Boron. Sample mass of 10.25 mg; ^{4}He cryostat. Data in order of measurement.

T/K	C_p/J K^{-1} mol^{-1}	T/K	C_p/J K^{-1} mol^{-1}	T/K	C_p/J K^{-1} mol^{-1}	T/K	C_p/J K^{-1} mol^{-1}
96.24	1.03	31.32	0.0692	9.99	0.00525	145.55	2.88
96.17	1.03	31.31	0.0695	9.99	0.00453	145.78	2.90
96.14	1.03	31.33	0.0701	9.99	0.00456	145.79	2.89
86.34	0.787	27.95	0.0561	8.91	0.00346	167.97	3.97
86.29	0.784	27.94	0.0547	8.91	0.00338	168.19	3.98
86.29	0.784	27.94	0.0553	8.91	0.00337	168.20	3.98
77.57	0.600	24.93	0.0436	7.95	0.00258	190.50	5.16
77.53	0.598	24.92	0.0434	7.95	0.00244	190.68	5.16
77.54	0.597	24.92	0.0436	7.95	0.00243	190.69	5.15
69.64	0.447	22.24	0.0345	7.09	0.00183	212.99	6.30
69.68	0.448	22.23	0.0345	7.09	0.00178	213.08	6.32
69.68	0.447	22.24	0.0342	7.09	0.00175	213.13	6.32
62.16	0.343	19.86	0.0270	6.35	0.00127	235.32	7.53
62.13	0.340	19.85	0.0268	6.34	0.00135	235.47	7.51
62.14	0.340	19.85	0.0269	6.34	0.00127	235.49	7.51
55.46	0.254	17.70	0.0218	5.64	0.000897	257.72	8.57
55.43	0.252	17.70	0.0210	5.64	0.000924	257.84	8.58
55.44	0.252	17.70	0.0207	5.64	0.000844	257.89	8.56
49.47	0.191	15.77	0.0165	5.03	0.000632	280.08	9.61
49.44	0.190	15.77	0.0157	5.03	0.000616	280.24	9.54
49.46	0.190	15.78	0.0157	5.03	0.000635	280.24	9.52
44.11	0.148	14.07	0.0123	4.00	0.000348	302.46	10.33
44.12	0.145	14.07	0.0123	3.57	0.000229	302.59	10.23
44.12	0.145	14.07	0.0123	3.57	0.000255	302.59	10.22
39.36	0.116	12.55	0.00965	101.08	1.18		
39.36	0.112	12.55	0.00884	101.04	1.18		
39.36	0.112	12.55	0.00873	101.04	1.18		
35.12	0.0884	11.19	0.00682	123.42	1.95		
35.11	0.0865	11.19	0.00681	123.43	1.95		
35.10	0.0877	11.19	0.00686	123.44	1.95		

Table SA4. Heat capacity of α-Boron. Sample mass of 10.18 mg; ^{4}He cryostat. Data in order of measurement.

T/K	C_p/J K^{-1} mol^{-1}	T/K	C_p/J K^{-1} mol^{-1}	T/K	C_p/J K^{-1} mol^{-1}	T/K	C_p/J K^{-1} mol^{-1}
4.18	0.000322	16.65	0.0192	58.25	0.317	202.07	5.70
4.75	0.000481	18.85	0.0257	66.02	0.427	222.03	6.77
5.38	0.000833	18.87	0.0259	66.04	0.428	222.22	6.77
5.38	0.000858	18.87	0.0259	66.02	0.429	222.24	6.76
6.09	0.00120	21.38	0.0344	74.79	0.582	242.18	7.83
6.09	0.00122	21.40	0.0345	74.83	0.584	242.37	7.79
6.10	0.00122	21.39	0.0345	74.83	0.584	242.37	7.78
6.90	0.00170	24.26	0.0453	84.77	0.790	262.23	8.79
6.91	0.00181	24.26	0.0455	84.82	0.794	262.42	8.74
6.91	0.00170	24.26	0.0457	84.82	0.793	262.42	8.73
7.82	0.00243	27.49	0.0595	96.04	1.07	282.50	9.73
7.84	0.00231	27.50	0.0599	96.10	1.08	282.65	9.68
7.83	0.00237	27.49	0.0596	96.11	1.07	282.66	9.66
8.88	0.00324	31.16	0.0775	101.20	1.22	302.66	10.48
8.89	0.00352	31.20	0.0752	101.19	1.22	302.79	10.42
8.89	0.00375	31.16	0.0774	101.18	1.22	302.79	10.42
10.07	0.00487	35.33	0.104	121.24	1.90		
10.08	0.00542	35.34	0.101	121.37	1.91		
10.08	0.00539	35.31	0.101	121.38	1.91		
11.42	0.00736	40.06	0.134	141.41	2.71		
11.43	0.00738	40.05	0.135	141.54	2.72		
11.43	0.00730	40.03	0.135	141.55	2.72		
12.93	0.00982	45.38	0.176	161.57	3.64		
12.95	0.0103	45.39	0.177	161.71	3.67		
12.95	0.0103	45.37	0.177	161.73	3.67		
14.67	0.0140	51.42	0.234	181.72	4.67		
14.68	0.0141	51.43	0.235	181.88	4.67		
14.68	0.0140	51.41	0.236	181.89	4.69		
16.63	0.0188	58.26	0.315	201.88	5.72		
16.64	0.0193	58.27	0.317	202.06	5.72		

Appendix B: Heat Capacity of β-Boron.

Table SB1. Heat capacity of β-Boron. Sample mass of 5.26 mg. Data in order of measurement.

T / K	C_p/J K^{-1} mol^{-1}
254.41	9.17
254.23	9.17
254.20	9.16
271.65	10.1
271.77	10.1
271.79	10.0
289.54	10.9
289.64	10.9
289.65	10.9

Table SB2. Heat capacity of β-Boron. Sample mass of 5.26 mg. Data in order of measurement.

T / K	C_p/J K^{-1} mol^{-1}
102.07	1.19
102.07	1.18
102.14	1.20
122.40	1.97
122.42	1.97
122.45	2.00
142.74	2.94
142.78	2.94
142.83	2.96
163.07	4.01
163.08	4.02
163.12	4.04
183.35	5.19
183.40	5.18
183.42	5.21
203.68	6.33
203.73	6.34
203.74	6.34
223.94	7.58
224.00	7.58
224.00	7.59
244.23	8.72
244.24	8.70
244.30	8.70
264.51	9.76
264.54	9.80
264.59	9.79
284.69	10.92
284.80	10.87
284.84	10.92

Table SB3. Heat capacity of β-Boron. Sample mass of 14.95 mg. Data in order of measurement.

T / K	C_p/J K^{-1} mol^{-1}	T / K	C_p/J K^{-1} mol^{-1}
49.96	0.123	122.45	2.03
49.96	0.124	142.70	2.97
49.96	0.123	142.73	2.97
55.79	0.180	142.81	2.98
55.80	0.181	162.98	4.05
55.80	0.179	163.02	4.05
62.31	0.266	163.10	4.05
62.31	0.266	183.27	5.21
62.31	0.268	183.32	5.20
69.60	0.375	183.39	5.20
69.60	0.375	203.55	6.36
69.61	0.379	203.60	6.36
77.71	0.540	203.64	6.36
77.72	0.541	223.82	7.57
77.72	0.545	223.86	7.56
86.78	0.757	223.87	7.55
86.79	0.758	244.07	8.66
86.81	0.764	244.08	8.66
96.91	1.06	244.10	8.67
96.91	1.06	264.33	9.74
96.95	1.06	264.35	9.75
102.02	1.22	264.37	9.75
102.04	1.22	284.50	10.8
102.11	1.23	284.59	10.8
122.36	2.02	284.61	10.8
122.38	2.01		

Table SB4. Heat capacity of β-Boron. Sample mass of 20.05 mg. Data in order of measurement.

T / K	C_p/J K^{-1} mol^{-1}	T / K	C_p/J K^{-1} mol^{-1}
37.09	0.0395	102.09	1.21
41.28	0.0580	102.22	1.22
41.28	0.0574	124.66	2.11
41.30	0.0573	124.72	2.11
45.94	0.0854	124.86	2.12
45.95	0.0863	147.23	3.20
45.96	0.0854	147.28	3.20
51.12	0.126	147.40	3.21
51.13	0.126	169.78	4.43
51.13	0.126	169.83	4.43
63.28	0.270	169.93	4.43
63.28	0.269	192.29	5.73
63.31	0.272	192.33	5.73
70.42	0.384	192.42	5.73
70.43	0.384	214.81	7.03
70.45	0.387	214.86	7.02
78.34	0.544	214.90	7.02
78.34	0.545	237.30	8.36
78.37	0.548	237.33	8.35
87.14	0.758	237.34	8.34
87.14	0.758	259.81	9.56
87.18	0.764	259.82	9.55
96.94	1.05	259.84	9.57
96.95	1.05	282.26	10.7
96.98	1.05	282.31	10.7
102.07	1.21	282.33	10.7

Table SB5. Heat capacity of β-Boron. Sample mass of 20.05 mg. Data in order of measurement.

T / K	C_p/J K^{-1} mol^{-1}
251.99	9.03
252.00	9.03
252.00	9.03
271.86	10.1
271.98	10.1
271.97	10.1
292.10	11.0
292.18	11.0
292.17	11.0

Table SB6. Heat capacity of β-Boron. Sample mass of 37.57 mg. Data in order of measurement.

T / K	C_p/J K^{-1} mol^{-1}	T / K	C_p/J K^{-1} mol^{-1}	T / K	C_p/J K^{-1} mol^{-1}	T / K	C_p/J K^{-1} mol^{-1}	T / K	C_p/J K^{-1} mol^{-1}	T / K	C_p/J K^{-1} mol^{-1}
2.02	0.0000528	5.02	0.000165	13.94	0.00242	38.73	0.0467	96.07	1.00	262.25	9.68
2.02	0.0000536	5.62	0.000227	13.94	0.00244	38.74	0.0467	101.11	1.16	262.27	9.68
2.02	0.0000539	5.62	0.000230	15.62	0.00326	38.75	0.0471	101.12	1.17	282.33	10.7
2.26	0.0000570	5.62	0.000222	15.63	0.00326	43.39	0.0694	101.27	1.17	282.34	10.7
2.27	0.0000572	6.31	0.000325	15.63	0.00326	43.40	0.0695	121.27	1.94	282.35	10.7
2.27	0.0000566	6.31	0.000310	17.50	0.00439	43.43	0.0701	121.28	1.94		
2.54	0.0000591	6.31	0.000313	17.51	0.00439	48.61	0.104	121.46	1.94		
2.54	0.0000583	7.04	0.000408	17.51	0.00440	48.63	0.104	141.44	2.88		
2.54	0.0000584	7.05	0.000400	19.62	0.00594	48.66	0.105	141.46	2.88		
2.84	0.0000643	7.05	0.000403	19.62	0.00594	54.47	0.157	141.67	2.88		
2.84	0.0000633	7.90	0.000551	19.64	0.00596	54.48	0.157	161.59	3.95		
2.84	0.0000656	7.91	0.000554	21.96	0.00810	54.52	0.159	161.60	3.95		
3.18	0.0000690	7.91	0.000554	21.97	0.00809	61.01	0.235	161.79	3.95		
3.19	0.0000681	8.85	0.000741	21.97	0.00812	61.02	0.235	181.74	5.10		
3.19	0.0000685	8.85	0.000736	24.60	0.0112	61.05	0.237	181.75	5.10		
3.57	0.0000862	8.85	0.000742	24.60	0.0112	68.35	0.341	181.91	5.10		
3.57	0.0000848	9.92	0.000992	24.61	0.0113	68.35	0.341	201.91	6.25		
3.57	0.0000793	9.92	0.000992	27.56	0.0155	68.40	0.343	201.91	6.26		
3.99	0.000108	9.93	0.000989	27.56	0.0156	76.55	0.499	202.03	6.27		
4.00	0.000110	11.10	0.00134	27.57	0.0157	76.55	0.499	222.04	7.45		
4.00	0.000104	11.11	0.00134	30.87	0.0221	76.62	0.502	222.05	7.45		
4.48	0.000131	11.11	0.00133	30.88	0.0222	85.73	0.710	222.16	7.46		
4.48	0.000137	12.44	0.00180	30.88	0.0223	85.73	0.712	242.13	8.58		
4.48	0.000122	12.45	0.00179	34.58	0.0318	85.81	0.714	242.14	8.58		
5.02	0.000182	12.45	0.00180	34.59	0.0317	96.06	1.00	242.20	8.58		
5.02	0.000174	13.94	0.00243	34.60	0.0329	96.06	1.00	262.24	9.68		

Table SB7. Heat capacity of β-Boron. Sample mass of 31.62 mg. Data in order of measurement.

T / K	C_p/J K^{-1} mol^{-1}	T / K	C_p/J K^{-1} mol^{-1}	T / K	C_p/J K^{-1} mol^{-1}
2.55	0.0000550	43.47	0.0664	121.37	1.90
2.55	0.0000539	48.64	0.0993	121.53	1.90
2.55	0.0000550	48.66	0.0993	141.54	2.83
2.85	0.0000566	48.67	0.100	141.54	2.83
2.85	0.0000574	54.49	0.150	141.70	2.83
2.86	0.0000555	54.51	0.150	161.72	3.88
3.19	0.0000675	54.52	0.152	161.72	3.88
3.20	0.0000680	61.05	0.225	161.85	3.89
3.20	0.0000644	61.06	0.225	181.88	5.01
24.63	0.00989	61.09	0.227	181.88	5.01
24.63	0.00990	68.39	0.332	181.99	5.02
24.64	0.00997	68.40	0.332	202.04	6.17
27.58	0.0141	68.43	0.335	202.04	6.17
27.59	0.0141	76.61	0.483	202.16	6.17
27.59	0.0142	76.61	0.485	222.19	7.34
30.90	0.0203	76.64	0.487	222.20	7.34
30.91	0.0201	85.80	0.693	222.28	7.34
30.91	0.0205	85.82	0.691	242.33	8.47
34.61	0.0293	85.87	0.697	242.34	8.47
34.62	0.0294	96.11	0.977	242.38	8.46
34.62	0.0295	96.11	0.978	262.45	9.54
38.76	0.0438	96.12	0.978	262.46	9.54
38.78	0.0439	101.17	1.13	262.47	9.54
38.78	0.0442	101.17	1.14	282.57	10.6
43.43	0.0657	101.30	1.14	282.59	10.6
43.44	0.0658	121.37	1.90	282.59	10.6

Table SB8. Heat capacity of β-Boron. Sample mass of 35.64 mg. Data in order of measurement.

T / K	C_p/J K^{-1} mol^{-1}	T / K	C_p/J K^{-1} mol^{-1}	T / K	C_p/J K^{-1} mol^{-1}
11.13	0.00120	27.60	0.0145	76.61	0.491
11.13	0.00120	30.89	0.0206	76.67	0.493
11.14	0.00120	30.91	0.0208	85.80	0.699
12.46	0.00157	30.92	0.0208	85.81	0.700
12.47	0.00157	34.61	0.0300	85.91	0.700
12.47	0.00159	34.61	0.0300	96.11	0.988
13.96	0.00209	34.63	0.0303	96.12	0.987
13.97	0.00209	38.77	0.0450	96.21	0.989
13.97	0.00209	38.78	0.0449		
15.64	0.00277	38.79	0.0467		
15.64	0.00277	43.42	0.0673		
15.65	0.00281	43.43	0.0673		
17.52	0.00377	43.45	0.0681		
17.52	0.00378	48.65	0.101		
17.53	0.00383	48.66	0.101		
19.63	0.00517	48.69	0.102		
19.63	0.00519	54.48	0.153		
19.64	0.00517	54.50	0.154		
21.99	0.00710	54.53	0.155		
21.99	0.00712	61.04	0.229		
22.01	0.00719	61.05	0.229		
24.63	0.0100	61.08	0.231		
24.63	0.0100	68.38	0.338		
24.65	0.0101	68.39	0.337		
27.58	0.0143	68.42	0.340		
27.59	0.0143	76.60	0.491		

Table SB9. Heat capacity of β-Boron. Sample mass of 35.64 mg. Data in order of measurement.

T / K	C_p/J K^{-1} mol^{-1}
11.04	0.00121
11.04	0.00120
11.06	0.00120
13.08	0.00179
13.08	0.00179
13.10	0.00182
15.49	0.00278
15.49	0.00279
15.51	0.00281
18.33	0.00437
18.34	0.00437
18.36	0.00444
21.70	0.00696
21.71	0.00696
21.73	0.00715
25.70	0.0115
25.71	0.0115
25.73	0.0118
30.44	0.0197
30.45	0.0196
30.48	0.0201
36.04	0.0355
36.05	0.0353
36.07	0.0354
42.65	0.0635
42.72	0.0628
42.73	0.0661
50.42	0.116
50.45	0.119
50.52	0.117

Table SB10. Heat capacity of β-Boron. Sample mass of 31.62 mg. Data in order of measurement.

T / K	C_p/J K^{-1} mol^{-1}	T / K	C_p/J K^{-1} mol^{-1}	T / K	C_p/J K^{-1} mol^{-1}
14.62	0.00247	39.94	0.0520	121.24	1.93
14.62	0.00248	45.26	0.0790	121.25	1.93
14.63	0.00249	45.27	0.0790	141.11	2.84
16.58	0.00346	45.31	0.0797	141.35	2.86
16.58	0.00346	51.29	0.125	141.37	2.86
16.59	0.00347	51.30	0.125	161.32	3.92
18.80	0.00489	51.35	0.126	161.56	3.93
18.80	0.00490	58.15	0.196	161.57	3.92
18.81	0.00494	58.17	0.196	181.44	5.05
21.32	0.00697	58.21	0.198	181.66	5.06
21.32	0.00697	65.93	0.300	181.67	5.07
21.33	0.00703	65.94	0.300	201.68	6.19
24.16	0.00993	66.00	0.302	201.80	6.24
24.17	0.00997	74.75	0.459	201.84	6.20
24.19	0.01000	74.76	0.458	221.69	7.27
27.40	0.0144	74.83	0.462	221.82	7.36
27.41	0.0144	84.71	0.682	221.87	7.31
27.42	0.0146	84.71	0.682	242.03	8.51
31.05	0.0218	84.80	0.685	242.03	8.51
31.05	0.0216	96.04	0.993	242.04	8.51
31.07	0.0217	96.05	0.992	262.12	9.57
35.21	0.0322	96.05	0.993	262.23	9.58
35.22	0.0322	101.08	1.16	262.23	9.58
35.22	0.0326	101.09	1.16	282.14	10.6
39.91	0.0504	101.18	1.16	282.23	10.6
39.92	0.0504	121.23	1.93	282.23	10.6

References Cited:

1. D. Ağaoğullari, Ö. Balci, İ. Duman, M. Lütfi Öveçoğlu, Synthesis of α- and β-rhombohedral boron powders via gas phase thermal dissociation of boron trichloride by hydrogen. *Metall. Mater. Trans. B* **42B**, 568-574 (2011).
2. G. Parakhonskiy, N. Dubrovinskaia, E. Bykova, R. Wirth, L. Dubrovinsky, Experimental pressure-temperature phase diagram of boron: resolving the long-standing enigma. *Sci. Rep*.**1**, 96:1-7 (2011).
3. O. O. Kurakevycha, Y. Le Godec, T. Hammouda, C. Goujon. Comparison of solid state crystallization of boron polymorphs at ambient and high pressures. arXiv:1110.1731 [cond-mat.mtrl-sci] (2011).
4. B. F. Decker, J. S. Kasper, *Acta Cryst*. 12, 503-506 (1959).
5. D. Geist, R. Kloss, H. Follner, *Acta Cryst*. B26, 1800-1804 (1970).
6. Quantum Design, *Physical Property Measurement System Resistivity Option User's Manual* (Quantum Design, San Diego, 1999).
7. C. A. Kennedy, M. Stancescu, R. A. Marriott, M. A. White, Recommendations for accurate heat capacity measurements using a Quantum Design physical property measurement system. *Cryogenics* **47**, 107-112 (2007).
8. V. N. Naumov *et al*., Heat capacity, thermodynamic functions, and density characteristics of the phonon states of α-rhombohedral boron. *Zhurnal Fizicheskoi Kimimii* **71**, 1596-1601 (1997).
9. G. V. Tsagareishvilli *et al*., in *Abstr. All-Union Conf. on Calorimetry and Chemical Thermodnamics*, Moscow, Moscow State University, Moscow, 1984, as quoted in D. Sh. Tsagareishvili *et al*., *J. Less Common Met.* **117**, 143-151 (1986).
10. Y. Kong *et al*., Elastic and thermodynamic properties of the Ni–B system studied by first-principles calculations and experimental measurements. *CALPHAD* **34**, 245-251 (2010).
11. A. Magnus, H. Danz, Specific heat of tungsten, boron, boron nitride and beryllium. *Ann. Phys*. **81**, 407-U14 (1926).
12. W. H. Evans, E. J. Prosen, D. D. Wagman, Thermochemistry and thermodynamic functions of some boron compounds. *Nat. Bur. Std. Report No*. 6252, Sept. 15, 1958, p. 226-235.
13. H. L. Johnston, H. N. Hersh, E. C. Kerr, Low-temperature heat capacities of inorganic solids. V. The heat capacity of pure elementary boron in both amorphous and crystalline conditions between 13 and 305°K. Some free energies of formation. *J. Am. Chem. Soc*. **73**, 1112-1117 (1951).
14. P. R. H. Türkes, E. T. Swartz, R. O. Pohl, Thermal properties of boron and boron carbides. *AIP Conf. Proc*. **140**, 346-361(1991).
15. V. I. Bogdanov *et al*., Temperature function of the specific heat of β-rhombohedral boron. *Fizika Tverdogo Tela* **12**, 3333-3336 (1970).
16. N. Bilir, W. A. Phillips, T. H. Geballe, Thermal properties of boron phases. *Proc. 14th International Conf. on Low-Temp Physics: Otaniemi, Finland*, **3**, 9-12 (1975).
17. Q. Hu, *et al*., Low-temperature specific heat of isotopically modified boron single crystals. *J. Appl. Phys*. **90**, 728-732 (2001).
18. M. W. Chase, *J. Phys. Chem. Ref. Data*, Monograph 9, NIST-JANAF Thermochemical Tables, 178 (1998).

19. S. R. Wise, J. L. Margrave, R. L. Altman, The heat content of boron at high temperatures. *J. Phys. Chem*. **64**, 915-917 (1960).
20. R. A. McDonald, D. R. Stull, Heat content and heat capacity of crystalline Boron from 298° to 1700° K. *J. Chem. Eng. Data* **7**, 84 (1962).
21. N. D. Stout, R. W. Mar, W. O. J. Boo, The high temperature enthalpy and the enthalpy of fusion of boron by drop calorimetry. *High Temp. Sci*. **5**, 241-251 (1973).
22. J. Sh. Jobova, G. I. Kalandadze, P. J. Kervalishvili, Chemical activity of elementary boron. *AIP Conf. Proc*. **231**, 542-549 (1991).
23. D. Sh. Dzhobava, G. I. Kalandadze, Chemical activity of elemental boron. *Inorg. Mater*. **26**, 1788-1790 (1990).
24. O. Madelung, U. Rössler, M. Shulz, Eds., *Landolt-Börnstein New Series*, Condensed Matter (Group III). Semiconductors, V. 041C, p. 59 (1998).
25. S. Hoffmann, H. Werheit, Phase transition in β-rhombohedral boron at 550 K. *Solid State Sci.* **14**, 1572 (2012).
26. D. Sh. Tsagareishvili, G. V. Tsagareishvili, I. S. Omiadze, J. Sh. Jobava, Thermodynamic properties of α-rhombohedral boron from 16.05 to 7.14 K. *J. Less-Common Met*. **117**, 143-151 (1986).
27. R. A. Cowley, Anharmonic crystals. *Reports on Progress in Physics* **31**, 123-166 (1968).
28. E.I. Andritsos *et al*., The heat capacity of matter beyond the Dulong-Petit value. *J. Phys.: Cond. Matter* **25**, 235410:1-6 (2013).
29. NIST Chemistry Web Book: http://webbook.nist.gov/chemistry/
30. P. Runow, Study of the α to β transformation in boron. *J. Mater. Sci*. **7** 499-511 (1972).
31. T. G. Dzhandieri, G. I. Kalandadze, P. D. Kervalishvili, Calorimetric study of phase changes in boron. *Inorg. Mater*. **24**, 1702-1704 (1988).
32. V. L. Solozhenko, O. O. Kurakevych, Equilibrium p-T phase diagram of boron: experimental study and thermodynamic analysis. *Sci. Rep.* **3**, 2351:1-8 (2013).
33. M. R. Ranade *et al*., Energetics of nanocrystalline TiO_2. *Proc. Nat. Acad. Sc*. **99**, 6476-6481 (2002).
34. W. Hayami and S. Otani, The role of surface energy in the growth of boron crystals. *J. Phys. Chem. C* **111**, 688-692 (2007).
35. B. Albert, H. Hillebrecht, Boron: elementary challenge for experimenters and theoreticians. *Angew. Chem*. **48**, 8640-8668 (2009).
36. J. Qin *et al*., Phase relations in boron at pressures up to 18 GPa and temperatures up to 2200 ◦C. *Phys. Rev. B* **85,** 014107:1-6 (2012).
37. E. A. Ekimov, J. B. Lebed, V. A. Sidorov, S. G. Lyapin, High-pressure synthesis of crystalline boron in B-H system. *Phys. Stat. Solidi B* **250**, 721-725 (2013).
38. A. R. Oganov *et al*., Ionic high-pressure form of elemental boron. *Nature* **457**, 863-868 (2009).